Blocking of Frizzled Signaling With a Homologous Peptide Fragment of Wnt3a/Wnt5a Reduces Infarct Expansion and Prevents the Development of Heart Failure After Myocardial Infarction

Hilde Laeremans, Tilman M. Hackeng, Marc A.M.J. van Zandvoort, Victor L.J.L. Thijssen, Ben J.A. Janssen, Harry C.J. Ottenheijm, Jos F.M. Smits and W. Matthijs Blankesteijn

Circulation 2011, 124:1626-1635: originally published online September 19, 2011
doi: 10.1161/CIRCULATIONAHA.110.976969
Circulation is published by the American Heart Association. 7272 Greenville Avenue, Dallas, TX 72514
 Print ISSN: 0009-7322. Online ISSN: 1524-4539

Blocking of Frizzled Signaling With a Homologous Peptide Fragment of Wnt3a/Wnt5a Reduces Infarct Expansion and Prevents the Development of Heart Failure After Myocardial Infarction

Hilde Laeremans, PhD; Tilman M. Hackeng, PhD; Marc A.M.J. van Zandvoort, PhD; Victor L.J.L. Thijssen, PhD; Ben J.A. Janssen, PhD; Harry C.J. Ottenheijm, PhD; Jos F.M. Smits, PhD; W. Matthijs Blankesteijn, PhD

Background—The molecular pathways that control the wound healing after myocardial infarction (MI) are not completely elucidated. One of these pathways is the Wnt/Frizzled pathway. In this study, we evaluated Frizzled as a novel therapeutic target for MI. These Frizzled proteins act as receptors for Wnt proteins and were previously shown to be expressed in the healing infarct.

Methods and Results—Wnt/Frizzled signaling has been studied for decades, but synthetic ligands that interfere with the interaction between Wnts and Frizzled have not been described to date. Here we report the selection of 3 peptides derived from regions of high homology between Wnt3a and Wnt5a that act as antagonists for Frizzled proteins. UM206, the peptide with the highest affinity, antagonized the effect of Wnt3a and Wnt5a in different in vitro assays. Administration of UM206 to mice for 5 weeks, starting immediately after the induction of MI, reduced infarct expansion and increased the numbers of capillaries and myofibroblasts in the infarct area. Moreover, heart failure development was inhibited by this therapy.

Conclusions—Blocking of Frizzled signaling reduces infarct expansion and preserves cardiac function after MI. Our findings underscore the potential of Frizzled receptors as a target for pharmacotherapy of cardiac remodeling after MI. **(*Circulation*. 2011;124:1626-1635.)**

Key Words: heart failure ■ myocardial infarction ■ myofibroblasts ■ pharmacology ■ receptor blocker ■ Wnt/frizzled pathway

The importance of Wnt signaling in developmental processes like cell proliferation, differentiation, and migration has been recognized for decades.[1,2] Wnt signaling has also been implicated in several diseases including cancer.[3,4] Although less well studied, there is growing evidence for a role of Wnt signaling in cardiovascular diseases, particularly in the remodeling that takes place in response to myocardial infarction (MI).[5–8] The underlying mechanism of Wnt signaling in cardiovascular diseases, however, is fundamentally different from that in, for example, colon cancer, in which mutations in the downstream signaling pathway lead to uncontrolled signaling and contribute to cell proliferation in the primary tumor. In cardiovascular diseases, no such mutations have been found to date. Instead, the increased expression of components of the Wnt signaling pathway suggests an activation rather than a disorder of the pathway.[7,8]

Clinical Perspective on p 1635

The involvement of Wnt signaling in multiple disease processes has fueled an intensive search for compounds that can modulate the activity of this pathway.[7,9–11] The major focus of this research has been on the signal transduction pathway where β-catenin acts as a second messenger. The degradation of β-catenin is controlled by a complex containing casein kinase I, glycogen synthase kinase 3β, axin, and adenomatous polyposis coli gene product.[4] Several well-known compounds can attenuate Wnt signaling, including LiCl, vitamins A and D, and nonsteroidal anti-inflammatory drugs.[10] Moreover, novel drugs that inhibit glycogen synthase

Received July 9, 2010; accepted July 5, 2011.

From the Departments of Pharmacology (H.L., B.J.A.J., H.C.J.O., J.F.M.S., W.M.B.), Biochemistry (T.M.H.), and Biomedical Engineering (M.A.M.J.v.Z.), Cardiovascular Research Institute Maastricht, Maastricht University, Maastricht, Netherlands; and Angiogenesis Laboratory, Department of Radiotherapy and Medical Oncology, VU Medical Center, Amsterdam, Netherlands (V.L.J.L.T.).

The online-only Data Supplement is available with this article at http://circ.ahajournals.org/lookup/suppl/doi:10.1161/CIRCULATIONAHA.110.976969/-/DC1.

Correspondence to W. Matthijs Blankesteijn, PhD, Department of Pharmacology and Toxicology, Cardiovascular Research Institute Maastricht, Maastricht University, 50 Universiteitssingel, 6229ER Maastricht/PO Box 616, 6200MD Maastricht, Netherlands. E-mail wm.blankesteijn@maastrichtuniversity.nl

Circulation **is available at http://circ.ahajournals.org** **DOI: 10.1161/CIRCULATIONAHA.110.976969**

kinase 3β or intervene in the interaction of β-catenin and T-cell factor/lymphoid enhancer factor have been described.[12] These compounds hold great promise for the treatment of cancer, in which β-catenin accumulation due to a defective degradation complex is a hallmark. However, in diseases characterized by an activated rather than a disordered Wnt signaling, like cardiovascular diseases, a direct intervention at the level of the Wnt receptor Frizzled (Fzd) appears to be preferable.

To activate signaling, Wnt proteins bind to a receptor complex formed by a member of the Fzd family and a low-density lipoprotein receptor–like protein.[13] This can evoke different intracellular responses, involving either β-catenin,[4] Ca^{2+}, or Rho kinase as a second messenger.[14] Apart from the interactions between Wnt3a/5a and Fzd-1 and -2, knowledge about the specific interplay between members of the Wnt (19 members) and Fzd (10 isoforms) families is limited,[13,15] and research on this topic has been hampered significantly by the lack of specific ligands.

The aim of the present study was to identify compounds that prevent the interaction between Wnts and Frizzled and to characterize their pharmacological and therapeutic properties. We focused on Fzd-1 and -2 because we have shown previously that these 2 Frizzled family members are upregulated in the infarcted heart. To this end, we selected regions of high homology between Wnt3a and Wnt5a that contain at least 2 cysteines. The presence of cysteines was considered to be advantageous to obtain a high binding affinity between peptide and receptor. Regions necessary for excretion or posttranslational modification of Wnt5a were excluded. This approach yielded 3 peptides, ranging from 13 to 22 amino acids in length. We tested their pharmacological properties in HEK293-TOPflash cells and immortalized cardiac fibroblasts and selected the peptide with highest affinity, UM206. We subsequently determined the pharmacokinetic properties of UM206 and studied the effect of UM206 administration on the wound-healing process after MI. Finally, we confirmed that the peptide fragment utilizes the Wnt3a binding site on Fzd-1 and -2.

Methods

Materials

The HEK superTOPflash cell line was kindly provided by J. Nathans, and CHO and COS-7 cells were obtained from DSMZ, Braunschweig, Germany. Cardiac fibroblasts immortalized with telomerase (CFIT) were developed and characterized in our laboratory.[16,17] The TOPflash construct was obtained from Upstate (Millipore, Billerica, MA). The peptides were synthesized in our laboratory, but large-scale synthesis of UM206 was performed by ChemPep, Miami, FL. Active caspase-3 antibody was obtained from Cell Signaling, Danvers, MA.

Cell Culture and Transient Transfection

CFIT were developed from primary rat cardiac fibroblasts by inducing stable overexpression of telomerase, as described previously.[17] All cells were cultured in 75-cm^2 culture flasks (Corning, Schiphol, Netherlands) in Dulbecco's modified essential medium with L-glutamine (2 mmol/L), 10% fetal calf serum (Invitrogen, Merelbeke, Belgium), and 1% gentamycin (Sigma-Aldrich, Zwijndrecht, Netherlands). Before the experiment was started, the cell lines were treated with plasmocin 25 μg/mL (Invivogen, Toulose, France) and tested with a MycoAlert mycoplasma detection kit (Lonza, Rockland, ME). Plasmid DNA was transiently transfected into the cells with the use of Fugene6 transfection reagent (Roche, Indianapolis, IN) DNA, according to the manufacturer's instructions. Fzd-1, -2, and -4 and Wnt3a and Wnt5a constructs cloned in pcDNA3.1/hygro (Invitrogen) and β-catenin and Fzd-5 constructs cloned in pcDNA3.0 (Invitrogen) were used. At 24 hours after transfection, conditioned culture medium, collected from either control L cells or L cells with Wnt3a or Wnt5a (Invitrogen) was added, either alone or in combination with antagonist.

Peptide Fragment Synthesis

All peptide fragments were synthesized by manual solid-phase peptide synthesis with the use of the in situ neutralization/activation procedure for Boc/Bzl peptide synthesis as described previously.[18] Please refer to the extended methods in the online-only Data Supplement for details.

Luciferase Experiments

For the luciferase experiments in cells that do not overexpress the TOPflash construct constitutively (ie, CHO and COS-7), transfection with a TOPflash construct (8 T-cell factor/lymphoid enhancer factor binding sites cloned into the pTA-Luc vector) was executed. Luciferase activity was measured with the use of a luciferase assay system (Promega, Madison, WI) according to the manufacturer's instructions.

Migration Assay

Cells were plated on day 0 and cultured until 70% confluence before transfection or treatment. Migration assays started 48 hours after transfection and/or treatment. The time point at which the scratch was made is indicated as 0 hours. Scratch width was measured at this time point and also after 6, 12, and 24 hours.[17]

Quantitative Polymerase Chain Reaction

RNA was isolated with the use of the Trizol method (Invitrogen). For the reverse transcription polymerase chain reaction, the RNA was transcribed to cDNA with iScript cDNA synthesis kit (Bio-Rad, Hercules, CA). Syber green (Eurogentec, Seraing, Belgium) was used for the detection of cDNA levels, and cyclophilin served as the housekeeping gene. In Table I in the online-only Data Supplement, the primer sequences are shown.

Western Blots

Western blotting was performed as described previously.[17] The following primary antibodies were used: β-catenin, α-smooth muscle actin (both 1:2000, BD Biosciences, Franklin Lakes, NJ), and β-actin (1:2000 Sigma-Aldrich). Anti-mouse immunoglobulin G 1/5000 (Vector Labs Inc) was used as the secondary antibody. Images of the blots were analyzed with image analysis software (Qwin Leica, Cambridge, United Kingdom).

Animal Surgery, Echocardiography, and Hemodynamic Analysis

Male Swiss mice were used (10–12 weeks of age; Charles River, Maastricht, Netherlands). This strain was previously found to show strong dilatation of the infarct area, frequently leading to heart failure. For the pharmacokinetic study, a venous cannula was implanted through which a bolus injection of UM206 was given, and blood samples were collected. For the treatment study, the animals were randomly included into the 3 different experimental groups. In the treatment study, either UM206 (6 μg/kg per day) or saline was administrated by an osmotic minipump (Alzet 2002 or 2006 for 2 and 5 weeks of treatment, respectively; Alzet, Cupertino, CA). We also tested an inactive analog of UM206 (CNKASEAMACEL) in the same dosage. MI was induced under isoflurane anesthesia, and echocardiography and hemodynamic analyses were performed as described previously[19]; please refer to the extended methods in the online-only Data Supplement for details. All experiments were

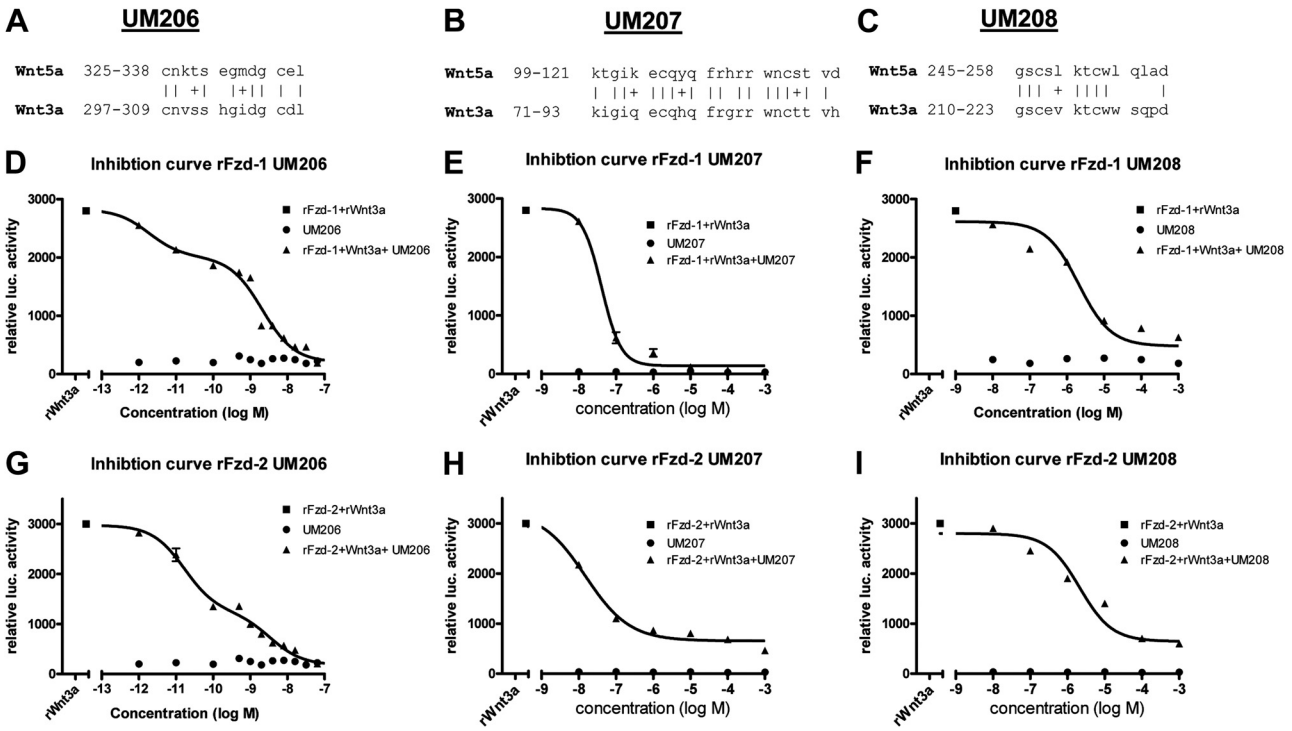

Figure 1. Characteristics of the Wnt5a-derived Frizzled (Fzd)-1 and -2 antagonists UM206, UM207, and UM208. **A** through **C**, Amino acid sequences of the 3 peptides, derived from Wnt5a, and their homology with Wnt3a. Identical amino acid residues are indicated by |; conserved substitutions are indicated by +. **D** through **I**, The inhibitory effects of UM206, UM207, and UM208 tested in an HEK superTOPflash cell line. The cells were transfected with either Fzd-1 or -2 as indicated and stimulated with Wnt3a (1 nmol/L) as indicated. All results are the average of 3 independent triplicate measurements and are represented as mean±SEM. See also Figure I and Table I in the online-only Data Supplement.

conducted according to international guidelines and approved by the Committee for Animal Research of Maastricht University.

High-Performance Liquid Chromatography

To determine the plasma concentration of UM206, reached by subcutaneous infusion with the minipumps, blood samples were collected from the animals after 14 to 35 days of treatment. Blood was centrifuged, and the plasma was treated with 1% trifluoroacetic acid. Analytical high-performance liquid chromatography was performed as described in the extended methods in the online-only Data Supplement.

Mass Spectrometry

Product-containing fractions were analyzed by electrospray ionization mass spectrometry, pooled, and lyophilized. Electrospray ionization mass spectrometry was performed on an Applied Biosystems SCIEX API 150 EX electrospray ionization quadrupole mass spectrometer. Peptide masses were calculated from the experimental mass to charge (m/z) ratios from all the protonation states observed in the electrospray ionization mass spectrometry spectrum of a peptide with the use of Analyst 1.4.2 software (Sciex, Warrington, UK).

Immunohistochemical Staining

One half of the hearts of the mice were embedded in paraffin and cut in 4-μm sections. The paraffin sections were rehydrated and washed in phosphate-buffered saline. Azan staining allowed an accurate determination of the infarct size. To visualize the myofibroblasts in the infarct area, the sections were incubated with an antibody directed against α-smooth muscle actin (Sigma-Aldrich), followed by incubation with the peroxidase-conjugated secondary antibody (Vector Laboratories). Nuclei were visualized by hematoxylin. Photos were taken with a Leica (CTR500, 63x/0.85) camera and analyzed with the Quantimet program (QWin/QGo, Leica, Cambridge, UK). An examiner blinded to the groups of the animals obtained all measurements. Blood vessels were stained with *Griffonia simplicifolia* I-B4 isolectin and quantified by counting the total amount of vessels in the infarct area. For the experiments with rhodamine-labeled UM206, frozen sections (4 μm) of mouse kidney and small intestine were used.

Statistical Analysis

All values are shown as mean±SEM. Statistical analyses were performed with the use of GraphPad Prism software. Differences between groups were examined for statistical significance with either 1- or 2-way ANOVA as appropriate with the Bonferroni posttest or unpaired Student *t* test. Survival curves were calculated with the use of the Kaplan-Meier method. Statistical analysis of the survival curves was performed with the log-rank test. A P value <0.05 was considered a statistically significant difference.

Results

Identification and Pharmacological Characterization of the Peptidergic Fzd Antagonists

In Figure 1A through 1C, the 3 regions of high homology between Wnt3a and Wnt5a that were selected are shown. We named the peptides UM206 through UM208. To determine the inhibitory constants of the peptides, HEK293-superTOPflash cells were transfected with either rFzd-1 or -2 and incubated with recombinant Wnt3a (1 nmol/L) in the presence of increasing concentrations of either of the peptides (Figure 1D through 1I). For UM206, a biphasic inhibition curve was observed that was best fitted with a 2–binding site model. In the cells transfected with rFzd-1 (Figure 1D), the

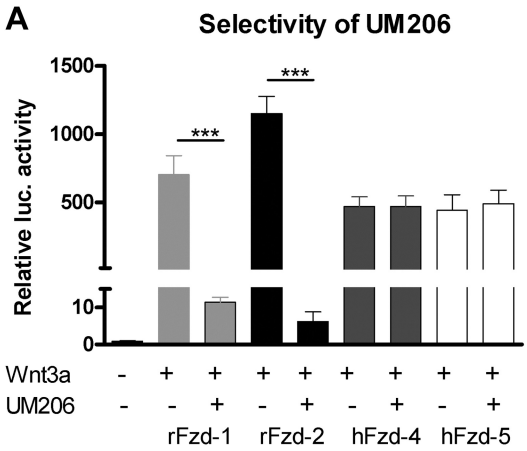

B **Structure activity relationships of UM206**

	% of inhibition for Fzd -1	*% of inhibition for Fzd -2*
Wnt3a	100 %	100 %
Wnt3a + UM206	28 %	15 %
Wnt3a + UM206 (1 C=A)	29 %	17 %
Wnt3a + UM206 (2 N =A)	32 %	20 %
Wnt3a + UM206 (3 K =A)	29 %	15 %
Wnt3a + UM206 (4 T=A)	**72 %**	**41 %**
Wnt3a + UM206 (5 S=A)	26 %	13 %
Wnt3a + UM206 (6 E=A)	29 %	15 %
Wnt3a + UM206 (7 G=A)	**47 %**	**37 %**
Wnt3a + UM206 (8 M=A)	32 %	15 %
Wnt3a + UM206 (9 D=A)	**59 %**	**49 %**
Wnt3a + UM206 (1 0 G=A)	30 %	17 %
Wnt3a + UM206 (1 1 C=A)	33 %	15 %
Wnt3a + UM206 (1 2 E=A)	34 %	14 %
Wnt3a + UM20 6 (13 L=A)	34 %	13 %
Wnt3a + UM206 (4 T=A, 7 G=A, 9 D=A)	**89 %**	**83 %**
Wnt3a + UM206 (C=A)	**100 %**	**92%**
Wnt3a + UM206 (C=C -alkyl)	**99 %**	**88 %**
Wnt3a + UM206 (C=S)	**100 %**	**83 %**
Wnt3a + UM206 (1-11)	**82 %**	**39 %**
Wnt3a + UM206 (12 -13 EL= AA)	**33 %**	**26 %**
Wnt3a +CNVSSHGIDGCDL	**55 %**	**38 %**

Figure 2. Selectivity and structure-activity relationships for UM206. **A**, Selectivity of UM206 for 4 different Frizzled (Fzd) receptors. These results indicate that UM206 at a concentration of 100 nmol/L specifically blocks Fzd-1 and -2. **B,** Essential amino acids for antagonistic activity of UM206 were determined by an Ala scan. Furthermore, some additional modifications of the Cys residues were tested. These results highlighted 4 important amino acids, namely, Cys, Thr, Asp, and Gly. Replacement of both Cys residues by Ala or Ser residues or alkylation of both Cys residues abolished the antagonistic properties of UM206. Simultaneous replacement of Thr, Asp, and Gly residues by Ala strongly reduced the antagonistic properties of UM206. The peptide CNVSSHGIDGCDL, derived from the area of Wnt3a homologous to UM206 (Figure 1A), also showed antagonistic properties, although the potency was lower than that of UM206. All results are the average of 3 independent measurements and are represented as mean±SEM (***$P<0.001$). Statistical test: Student *t* test.

high affinity site with an IC_{50} of $2.10\pm0.18\ 10^{-9}$ mol/L was most prominent, whereas in rFzd-2 transfected cells (Figure 1G), the binding site with an IC_{50} of $1.69\pm0.04\ 10^{-11}$ mol/L was the major binding site. This suggests that UM206 binds to rFzd-2 with ≈100-fold higher affinity than to rFzd-1. In contrast, the inhibition curves for UM207 and UM208 were best fitted with a single–binding site model; the IC_{50} values for Fzd-1 were $4.00\pm0.07\ 10^{-8}$ mol/L (Figure 1E) and $2.06\pm0.09\ 10^{-6}$ mol/L (Figure 1F) and for Fzd-2 $1.52\pm0.08\ 10^{-8}$ mol/L (Figure 1H) and $2.11\pm0.11\ 10^{-6}$ mol/L (Figure 1I) for UM207 and UM208, respectively. Administration of the peptides in the absence of Wnt3a had no effect on the luciferase activity. These results show that UM206 was the peptide with the highest affinity for rFzd-1 and -2, and therefore in the remainder of the experiments this antagonist was used.

Complete inhibition of the Wnt3a-induced luciferase activity with UM206-8 was also observed in CHO and COS-7 cells (Figure I in the online-only Data Supplement), although the fold induction of luciferase activity was considerably lower in these cells compared with HEK293-superTOPflash cells. Peptides derived from other regions of Wnt proteins showed no activity in concentrations up to 10 μmol/L (Table II in the online-only Data Supplement).

UM206 Blocks Fzd-1 and -2 But Not Fzd-4 and -5

In Figure 2A, the specificity of UM206 for Fzd-1 and -2 is shown. Addition of UM206 in a concentration of 100 nmol/L abolished the induction of luciferase activity almost completely in cells overexpressing rFzd-1 and -2 but had no effect on cells overexpressing hFzd-4 or -5. This was not due to species differences because UM206 was fully effective in antagonizing the activation of mouse and human Fzd-1 and -2 by Wnt3a as well (data not shown).

Structure-Activity Relationship of UM206

In Figure 2B, the effect of substitution of each of the individual amino acids of UM206 by Ala on the inhibition of Wnt3a-induced luciferase activity is shown. This Ala scan showed that replacement of Thr,[4] Gly,[7] and Asp[9] affected the inhibitory properties of UM206 most strongly. The combined replacement of these 3 amino acids by Ala residues abolished the antagonizing properties almost completely. Substitution of either of the Cys residues at position 1 or 11 did not affect the antagonistic effect of UM206, but simultaneous substitution of both Cys residues by either Ala or Ser rendered UM206 completely ineffective. Alkylation of both Cys residues had the same effect. Substitution of the C-terminal Glu and Leu by an Ala-Ala sequence reduced the inhibitory properties of UM206 only slightly, whereas deletion of the C-terminal Glu and Leu sequence led to a significant reduction of the potency of UM206. On the basis of these results, we propose that the antagonistic effect of UM206 is due to the presence of Thr, Gly, and Asp combined with at least 1 Cys residue. The peptide derived from the region of Wnt3a homologous to UM206 (Figure 1A) could also block the Wnt3a-induced effect but at a slightly lower efficacy than UM206.

UM206 Antagonized the Effects of Wnt3a and Wnt5a on Immortalized Cardiac Fibroblasts

The overexpression of Fzd-1 and -2 in migrating (myo)fibroblasts during infarct healing was one of the first reports of

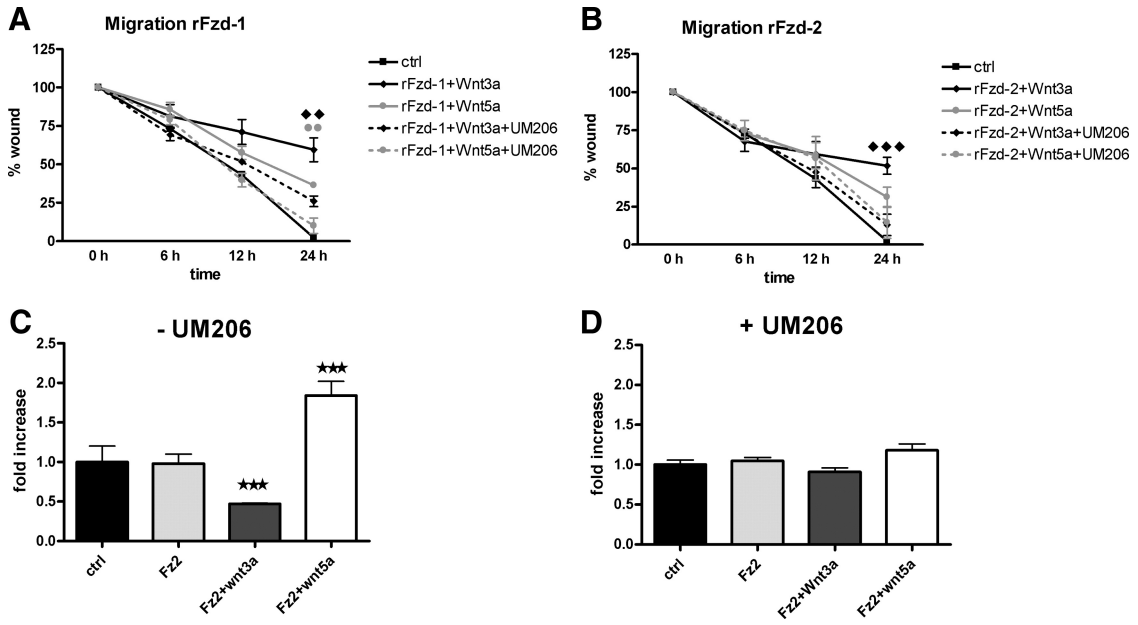

Figure 3. Wound assay, in which the migration of cardiac fibroblasts immortalized with telomerase (CFIT) into a scratch in the cell layer was studied under different conditions. Overexpression of Frizzled (Fzd)-1 (**A**) or -2 (**B**) alone or in combination with Wnt3a or Wnt5a significantly attenuated the CFIT migration. This attenuation of the migration could be counteracted by addition of UM206 (100 nmol/L). The effect of Wnt3a and Wnt5a on CFIT transfected with Fzd-2 is shown in **C**, as published previously by our group.[17] As shown in **D**, these effects can be blocked completely by addition of UM206 (10 nmol/L) to the culture medium. All results are the average of 3 independent triplicate measurements and are represented as mean±SEM (**$P<0.01$, ***$P<0.001$). Statistical test: **A** and **B**, 2-way ANOVA; **C** and **D**, 1-way ANOVA, both with Bonferroni correction. Ctrl indicates control.

activation of Wnt/Fzd signaling in cardiovascular remodeling.[20] To assess the functional relevance of Wnt/Fzd signaling on cardiac fibroblast proliferation, migration, and differentiation, CFIT were used, as described previously.[16,17] Administration of either Wnt3a or Wnt5a attenuated the migration of CFIT overexpressing either rFzd-1 or -2 (Figure 3A and 3B, respectively). These effects were blocked almost completely by addition of UM206 (100 nmol/L) to the culture medium. Next we investigated the effect on CFIT differentiation and found that UM206 could completely block the effects of both Wnt3a and Wnt5a (Figure 3C and 3D).

UM206 Reduced Ventricular Remodeling and Prevented Heart Failure Development After MI in Mice

To determine the pharmacokinetic properties of UM206, we injected 15 μg into the tail vein of mice and monitored the concentration in the blood at different time points. The half-life was 84±2 minutes (n=24; Figure II in the online-only Data Supplement). This half-life, combined with the high affinity of UM206, allowed us to test its effects on infarct healing in mice. To this end, we administered UM206 subcutaneously by an osmotic minipump (6 μg/kg per day); the control group was equipped with a saline-filled minipump. The minipumps were implanted at the time of infarct induction and lasted for up to 5 weeks. UM206 administration offered a dramatic improvement of survival: At 5 weeks after MI, 35% of the saline-treated mice had died, whereas all mice were still alive in the UM206-treated group (Figure 4A). Postmortem analysis revealed that the saline-treated animals died from heart failure, as diagnosed by a wet, foamy aspect of the lungs and severely elevated wet lung weight. In the surviving saline-treated mice, wet lung weight was 40% higher than in the UM206-treated mice at 5 weeks after MI, suggesting development of heart failure in the surviving saline-treated mice as well (Figure 4B). Echocardiography showed an improved ejection fraction and a 40% reduction in end-diastolic volume of the left ventricle in the UM206-treated compared with the saline-treated group, all indicative of a better preservation of cardiac function (Figure 4C1 and 4C2). Cardiac function was further assessed with the use of a Millar pressure recording catheter inserted into the left ventricle. The tangents on the pressure time curve were significantly steeper in the UM206-treated groups, resulting in a higher positive dP/dt and a lower negative dP/dt value (Figure 4D1 and 4D2), underscoring the positive effect of this treatment on cardiac function after MI. Similar beneficial effects were observed when UM206 treatment was started at 2 weeks after MI and continued until 5 weeks after MI (Figure III in the online-only Data Supplement). Finally, we tested CNKASEAMACEL, an inactive variant of UM206, in the infarct model to exclude nonspecific effects of peptide administration. The results in this group did not significantly differ from those of the saline-treated group.

UM206 Treatment Improved the Characteristics of the Infarct Area

UM206 treatment profoundly reduced infarct expansion and ventricular dilatation compared with saline treatment. This was confirmed by histological analysis of the infarct area (Figure 5A1 and 5A2). The infarct areas were significantly smaller in UM206-treated than saline-treated mice (Figure 5B) at both 2 and 5 weeks after MI. Moreover, as shown in Figure 5C, the infarct areas were significantly thicker in the UM206-treated mice at both time points. Myofibroblast

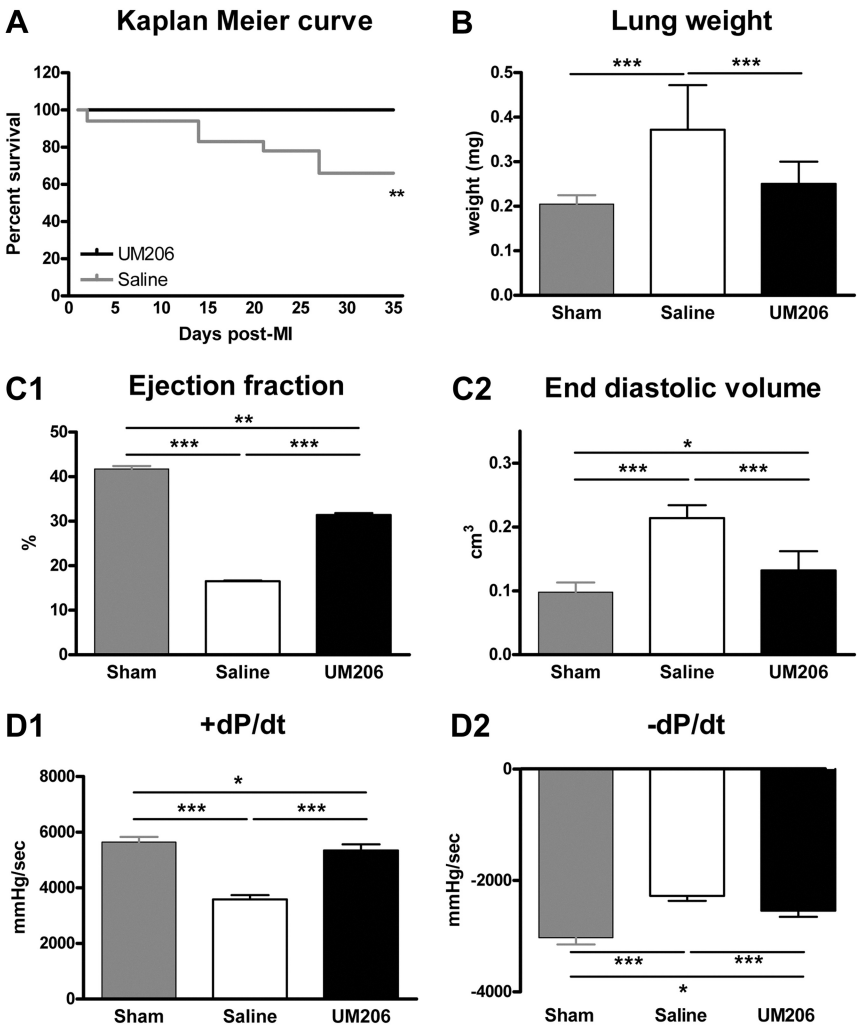

Figure 4. UM206 improves survival and reduces the deterioration of cardiac function after myocardial infarction (MI) in mice. **A**, Kaplan-Meier plot of the effect of UM206 treatment on the survival rate of mice in which MI was induced at t=0. UM206 treatment completely prevented the mortality after infarction, whereas in saline-treated mice the mortality was ≈35% after 5 weeks (n=18 animals per group). **B**, Increased lung weight in the saline-treated group is indicative of heart failure in the mice that survived for 5 weeks after MI. UM206 treatment significantly reduced this increase in lung weight. **C1** and **C2,** Echocardiographic measurements of ejection fraction and end-diastolic volume show improved cardiac function in the UM206-treated group. **D1** and **D2,** Hemodynamic measurements indicate that cardiac function was significantly better preserved after UM206 treatment compared with saline treatment. All data are represented as mean±SEM. Sample sizes in **B** through **D** were 18 in the UM206-treated and 12 in the saline group (*$P<0.05$, **$P<0.01$, ***$P<0.001$). See also Figure II in the online-only Data Supplement. Survival curves were calculated by the Kaplan-Meier method. Statistical analysis of the survival curves was performed with the log-rank test. Data in **B** through **D2** were analyzed with 1-way ANOVA with Bonferroni correction.

numbers were >4-fold higher in the UM206-treated mice at both time points (Figure 5D). The higher myofibroblast numbers in the UM206-treated group could be confirmed by significantly higher α-smooth muscle actin levels in the 5-week-old UM206-treated infarcts, as determined by quantitative polymerase chain reaction (Figure 5E1) and Western blotting (Figure 5E2). Moreover, UM206 treatment (5 weeks) resulted in an increase amount of blood vessels (Figure 5F) and reduced total collagen levels (Figure 5G) in the infarct area compared with saline treatment. Collagen Iα1 expression was significantly upregulated, whereas collagen III expression was significantly downregulated (Figure IV in the online-only Data Supplement). To further investigate whether UM206 has a direct effect on blood vessel formation, we analyzed its effects on human umbilical vein endothelial cell (HUVEC) differentiation and migration. UM206 by itself had no effect on either of these 2 processes and also did not affect the increased HUVEC proliferation induced by Wnt3a. The combination of Wnt3a and UM206 attenuated the HUVEC migration, whereas individually the compounds did not have a significant effect (Figure V in the online-only Data Supplement). These results suggest that UM206 does not have a direct stimulating effect on angiogenesis in the infarct area.

In our experiments, we did not observe any effects of UM206 on other organs known to contain Fzd-2, including kidney and small intestine. Quantitative polymerase chain reaction of several Wnt target genes revealed no difference in the expression levels of these genes in animals treated with UM206 for 5 weeks (Table III in the online-only Data Supplement). The difference in myofibroblast numbers could not be attributed to a difference in apoptosis, as determined by active caspase-3 immunohistochemistry (UM206 treated, 1.60±0.12%; saline treated, 1.83±0.75%). UM206 treatment caused a significant increase in Fzd-1 and -2 expression, whereas the expression of Wnt3a and Wnt5a was reduced in this group (Figures VI and VII in the online-only Data Supplement).

Blocking of Rhodamine-Labeled UM206 Binding by UM207 and Wnt3a

To demonstrate that the binding site of UM206 on Fzd is shared with UM207 and Wnt3a, we synthesized rhodamine-labeled UM206. Attachment of rhodamine to Lys^3 of UM206 did not affect its IC_{50} value for blocking Wnt3a-induced luciferase expression in HEK293 superTOPflash cells (not shown). As shown in Figure VIII in the online-only Data Supplement, incubation of frozen sections of mouse kidney and gut with UM206 rhodamine (10 nmol/L) for 15 minutes, followed by rinsing in ice-cold phosphate-buffered saline, revealed staining of tubular epithelium and villi as assessed

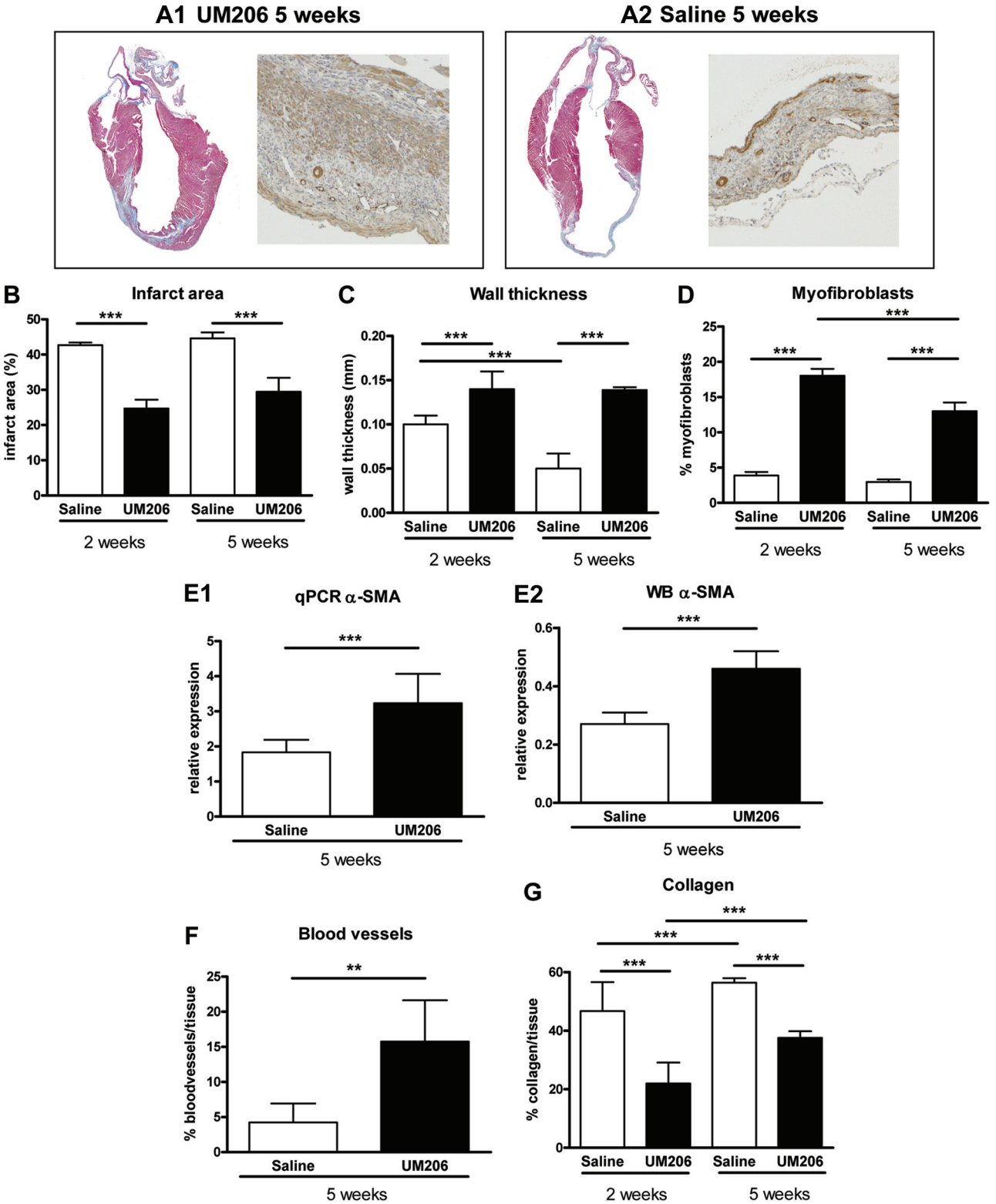

Figure 5. Characteristics of the infarct area in mice treated with UM206. **A1** and **A2,** Transverse sections of a UM206-treated and saline-treated heart, stained with hematoxylin-eosin. The infarcts were less expanded and thicker after UM206 treatment. Enlarged images represent myofibroblasts stained for α-smooth muscle actin (α-SMA). **B,** Infarct areas were smaller in the UM206-treated group after both 2 and 5 weeks. **C**, Wall thickness of the infarct area, however, was increased in UM206-treated mice. **D**, The infarct area of UM206-treated mice contained a 4-fold higher number of myofibroblasts. **E1** and **E2**, To support the histological data, α-smooth muscle actin content was determined both at RNA (quantitative polymerase chain reaction [qPCR]) and protein (Western blot [WB]) levels. These results confirm the immunohistochemical data, in which myofibroblast numbers were found to be increased after UM206 treatment. **F**, UM206 treatment increases the neovascularization of the infarct area, as reflected by an increased blood vessel/tissue area ratio. **G**, Collagen content was decreased after UM206 treatment. All results are the mean of 18 animals per group and are represented as mean±SEM (*$P<0.05$, **$P<0.01$, ***$P<0.001$). See also Table II in the online-only Data Supplement. Statistical analysis: Student *t* test.

by 2-photon microscopy. Specificity of the binding site was tested by prior incubation of the tissue sections with UM207 (100 nmol/L) or recombinant Wnt3a (10 nmol/L). Both compounds abolished the binding of UM206 rhodamine to its receptors but left the green autofluorescence of blood vessels unaffected. These data strongly suggest that UM206, UM207, and Wnt3a utilize a shared binding site on Fzd.

Discussion

In this article, we describe the identification of peptidergic Frizzled antagonists based on regions of high homology between Wnt3a and Wnt5a. Using predefined criteria, we identified UM206 through UM208, which all can block the activation of Fzd-1 and -2 by Wnt3a and Wnt5a. All 3 peptides feature 2 Cys residues, separated by 4 to 10 amino acids. Gly, Asp, and Thr residues are present in all 3 peptides and were shown to be important in the blocking effect of UM206. Because UM206 showed the highest affinity, we used this peptide in the remainder of the experiments. Either of the 2 Cys residues of UM206 could be replaced by Ala with little consequence for the binding, but replacing or blocking both Cys residues caused complete loss of activity. This may suggest a covalent interaction between a Cys residue of the compound and the Cys-rich domain of the receptor, which will be the subject of further study.

In our experiments, we observed that UM206 could block the effects of both Wnt3a and Wnt5a with high potency in different cell lines. Wnt3a can activate the canonical (β-catenin–mediated) pathway, whereas Wnt5a is generally believed to activate noncanonical Wnt signaling.[3] Moreover, we have shown previously that the effect of Wnt3a and Wnt5a on CFIT migration is through noncanonical signaling,[17] whereas the readout of the HEK superTOPflash cell line is directly linked to canonical Wnt signaling. Therefore, we conclude that UM206 can effectively antagonize both canonical and noncanonical Wnt signaling.

UM206 administration had a beneficial effect on infarct healing. It increased myofibroblast and blood vessel numbers in the infarct area, prevented infarct expansion, improved cardiac function, and completely prevented heart failure–related mortality. Thus far, the role of Wnt signaling in infarct healing has only been studied by genetic interventions. Barandon et al[21] were the first to show a beneficial effect of overexpression of FrzA, a bovine homologue of soluble Frizzled-related protein-1, on infarct healing. They observed a decreased infarct size with elevated numbers of myofibroblasts and blood vessels. Similar results were reported by Kobayashi et al[22] in mice lacking soluble Frizzled-related protein-2. However, in the latter study it was concluded that this was the result of a direct effect of soluble Frizzled-related protein-2 on procollagen-C-proteinase rather than blocking of Wnt signaling. This underscores that the role of soluble Frizzled-related proteins in infarct healing is complex and may not solely be the result of Wnt inhibition. We did not observe any adverse effects of long-term UM206 administration, indicating that this therapeutic intervention is safe and does not interfere with normal physiological processes.

In most of our in vivo experiments, we started the administration of UM206 directly after induction of the infarct. This raised the question of whether starting directly after infarction is critical for a beneficial effect. To investigate this, we started UM206 therapy at 2 weeks after MI in a separate group of mice and euthanized them at 5 weeks. The effect of this "late" treatment on hemodynamic parameters was similar to a full 5-week treatment (Figure III in the online-only Data Supplement). This observation is not only of importance for a potential therapeutic application of UM206 but also may suggest that the effect of UM206 is not primarily directed to the early phases of infarct healing (cardiomyocyte death and inflammatory response[23]).

The role of myofibroblasts in wound healing and tissue repair is well established. These cells are responsible for the contraction of skin wounds, thereby limiting the size of the scar that is formed at the site of injury.[24] More recently, a similar role has been described for myofibroblasts in the infarct area,[23,25–28] thereby preventing infarct expansion.[19,29] Moreover, myofibroblasts remain present in well-healed human infarcts for decades but are scarce in dilated infarcts obtained from heart failure patients.[30] Previously, we have shown that myofibroblasts express Fzd-1 and -2 during their migration into the infarct area.[20] Overexpression of components of the Wnt/Fzd pathway affects the differentiation and migration of CFIT.[17] Therefore, our data suggest that Fzd-1 and -2, expressed during infarct healing,[20] may play a functional role in the wound healing process after MI and may serve as a therapeutic target for intervention in this process. Moreover, the results of the present study may highlight the importance of increasing myofibroblast numbers to preserve cardiac function in the remodeling heart,[23,31] although we cannot exclude that UM206 targets other cell types in the healing infarct as well. UM206 may serve as a lead for the development of a novel drug class that addresses the process of infarct healing. This is of particular importance because the drugs that are currently available for the treatment of MI cannot prevent infarct expansion in all patients.[32]

UM206 therapy increased the blood vessel density in the infarct area. A role of Wnt signaling in blood vessel development has been reported previously by our group[33] and others,[34] and increased blood vessel formation was also observed in FrzA-overexpressing mice subjected to infarction.[21] To study a potential direct effect of UM206 on blood vessel formation, experiments with HUVEC were performed. UM206 by itself had no effect on HUVEC proliferation and migration. Moreover, UM206 could not block the Wnt3a-induced increase in HUVEC proliferation. On the other hand, the combination of UM206 and Wnt3a attenuated the HUVEC migration. Taken together, these data suggest that UM206 does not have a direct proangiogenic effect in the healing infarct. Interestingly, angiogenesis has been reported to be Fzd4 and Fzd5 dependent,[34] and UM206 was shown to have no effect on this Frizzled family member in the present study. A possible explanation for our observations is that the increase in vessel density in the infarct area may be secondary to the demand for oxygen and nutrients of the myofibroblasts in the infarct area, thereby improving the survival of these cells.

Previously, we studied the effects of activation of the Wnt/Frizzled pathway on CFIT in more detail.[17] In this study, we observed that migration of CFIT was reduced when

Wnt3a or Wnt5a was added to the culture medium, an effect that could be blocked completely with UM206. When we extrapolate this to our in vivo data, this mechanism may contribute to the increased myofibroblast numbers in the infarct area on UM206 treatment. Moreover, we observed a profound change in the relative expression levels of collagen Ia1 and collagen III in the UM206-treated animals (Figure IV in the online-only Data Supplement). Collagen I is known to resist distension better than collagen III,[35] which is likely to contribute to the better preservation of the left ventricular dimensions in the UM206-treated group.

Rhodamine-labeled UM206 was used to investigate the binding site of UM206 and UM207 on Fzd-1 and -2 in kidney and small intestine. The binding of rhodamine-labeled UM206 could be prevented by preincubation with either Wnt3a or UM207. These results strongly suggest that UM206, UM207, and Wnt3a occupy the same binding site on the Fzd-1 and -2 proteins. Therefore, the effects of UM206 and UM207 most likely can be attributed to competition with Wnts for binding to the Fzd-1 or -2 protein.

In the present study, we observed a beneficial effect on cardiac remodeling and function of UM206, and we tried to identify its mechanism of action by performing in vitro experiments. However, these experiments face several limitations. Our in vitro data suggest that myofibroblasts may be the most likely target of UM206, but these data were generated with the use of the immortalized cardiac fibroblast cell line CFIT, overexpressing either Fzd-1 or Fzd-2, as a model system. We could not use primary cultures of cardiac fibroblasts for this purpose because they differentiate spontaneously into myofibroblasts in culture and are difficult to transfect. Therefore, these experiments do not provide formal proof that (myo)fibroblasts in the infarct area are the only target of UM206 in vivo. We also observed an increase in blood vessel density in the infarct areas of UM206-treated mice. In the in vitro experiments with HUVEC, UM206 had no direct effect on endothelial cell proliferation and differentiation, but these data were generated with the use of untransfected cells and therefore may not be directly comparable to the CFIT data. Finally, we cannot rule out an effect of UM206 on the inflammatory response after MI. Therefore, additional experiments will be needed to draw firm conclusions regarding the target(s) and the mechanism of action of UM206 in the healing infarct.

In conclusion, the present study shows that fragments of Wnt proteins can serve as high-affinity Frizzled antagonists. Moreover, blocking of Frizzled can be a successful and safe approach to prevent infarct expansion. Specifically targeting the wound-healing process in the infarcted heart may serve as a novel and promising approach to prevent heart failure development in MI patients.

Acknowledgments

The authors acknowledge the skillful technical assistance of Agnieszka Brouns-Strzelecka, Lily Vervoort-Peters, Peter Lijnen, and Dennis Suylen.

Sources of Funding

This work was supported by BSIK grant 03033.

Disclosures

None.

References

1. Nelson WJ, Nusse R. Convergence of Wnt, beta-catenin, and cadherin pathways. *Science*. 2004;303:1483–1487.
2. van Gijn ME, Blankesteijn WM, Smits JF, Hierck B, Gittenberger-de Groot AC. Frizzled 2 is transiently expressed in neural crest-containing areas during development of the heart and great arteries in the mouse. *Anat Embryol (Berl)*. 2001;203:185–192.
3. Polakis P. The many ways of Wnt in cancer. *Curr Opin Genet Dev*. 2007;17:45–51.
4. MacDonald BT, Tamai K, He X. Wnt/beta-catenin signaling: components, mechanisms, and diseases. *Dev Cell*. 2009;17:9–26.
5. van Gijn ME, Daemen MJ, Smits JF, Blankesteijn WM. The Wnt-frizzled cascade in cardiovascular disease. *Cardiovasc Res*. 2002;55:16–24.
6. van de Schans VA, Smits JF, Blankesteijn WM. The Wnt/frizzled pathway in cardiovascular development and disease: friend or foe? *Eur J Pharmacol*. 2008;585:338–345.
7. Brade T, Manner J, Kuhl M. The role of Wnt signalling in cardiac development and tissue remodelling in the mature heart. *Cardiovasc Res*. 2006;72:198–209.
8. Blankesteijn WM, van de Schans VA, Ter Horst P, Smits JF. The Wnt/frizzled/GSK-3beta pathway: a novel therapeutic target for cardiac hypertrophy. *Trends Pharmacol Sci*. 2008;29:175–180.
9. Nusse R. Wnt signaling in disease and in development. *Cell Res*. 2005; 15:28–32.
10. Barker N, Clevers H. Mining the Wnt pathway for cancer therapeutics. *Nat Rev Drug Discov*. 2006;5:997–1014.
11. Safholm A, Leandersson K, Dejmek J, Nielsen CK, Villoutreix BO, Andersson T. A formylated hexapeptide ligand mimics the ability of Wnt-5a to impair migration of human breast epithelial cells. *J Biol Chem*. 2006;281:2740–2749.
12. Takahashi-Yanaga F, Sasaguri T. The Wnt/beta-catenin signaling pathway as a target in drug discovery. *J Pharmacol Sci*. 2007;104: 293–302.
13. Schulte G, Bryja V. The Frizzled family of unconventional G-protein-coupled receptors. *Trends Pharmacol Sci*. 2007;28:518–525.
14. Qu J, Zhou J, Yi XP, Dong B, Zheng H, Miller LM, Wang X, Schneider MD, Li F. Cardiac-specific haploinsufficiency of beta-catenin attenuates cardiac hypertrophy but enhances fetal gene expression in response to aortic constriction. *J Mol Cell Cardiol*. 2007;43:319–326.
15. Hendrickx M, Leyns L. Non-conventional Frizzled ligands and Wnt receptors. *Dev Growth Differ*. 2008;50:229–243.
16. Janhunen S, Laeremans H, Rensen S, Smits J, Blankesteijn W. Characterization of a cardiac fibroblast cell line immortalized with telomerase. *Naunyn Schmiedebergs Arch Pharmacol*. 2009;379:205.
17. Laeremans H, Rensen SS, Ottenheijm HC, Smits JF, Blankesteijn WM. Wnt/frizzled signalling modulates the migration and differentiation of immortalized cardiac fibroblasts. *Cardiovasc Res*. 2010;87: 514–523.
18. Schnolzer M, Alewood P, Jones A, Alewood D, Kent SB. In situ neutralization in Boc-chemistry solid phase peptide synthesis: rapid, high yield assembly of difficult sequences. *Int J Pept Protein Res*. 1992;40: 180–193.
19. van den Borne SW, van de Schans VA, Strzelecka AE, Vervoort-Peters HT, Lijnen PM, Cleutjens JP, Smits JF, Daemen MJ, Janssen BJ, Blankesteijn WM. Mouse strain determines the outcome of wound healing after myocardial infarction. *Cardiovasc Res*. 2009;84:273–282.
20. Blankesteijn WM, Essers-Janssen YP, Verluyten MJ, Daemen MJ, Smits JF. A homologue of *Drosophila* tissue polarity gene frizzled is expressed in migrating myofibroblasts in the infarcted rat heart. *Nat Med*. 1997;3: 541–544.
21. Barandon L, Couffinhal T, Ezan J, Dufourcq P, Costet P, Alzieu P, Leroux L, Moreau C, Dare D, Duplaa C. Reduction of infarct size and prevention of cardiac rupture in transgenic mice overexpressing FrzA. *Circulation*. 2003;108:2282–2289.
22. Kobayashi K, Luo M, Zhang Y, Wilkes DC, Ge G, Grieskamp T, Yamada C, Liu TC, Huang G, Basson CT, Kispert A, Greenspan DS, Sato TN. Secreted Frizzled-related protein 2 is a procollagen C proteinase enhancer with a role in fibrosis associated with myocardial infarction. *Nat Cell Biol*. 2009;11:46–55.
23. Sun Y, Kiani MF, Postlethwaite AE, Weber KT. Infarct scar as living tissue. *Basic Res Cardiol*. 2002;97:343–347.

24. Hinz B, Phan SH, Thannickal VJ, Galli A, Bochaton-Piallat ML, Gabbiani G. The myofibroblast: one function, multiple origins. *Am J Pathol*. 2007;170:1807–1816.
25. van den Borne SW, Diez J, Blankesteijn WM, Verjans J, Hofstra L, Narula J. Myocardial remodeling after infarction: the role of myofibroblasts. *Nat Rev Cardiol*. 2010;7:30–37.
26. Squires CE, Escobar GP, Payne JF, Leonardi RA, Goshorn DK, Sheats NJ, Mains IM, Mingoia JT, Flack EC, Lindsey ML. Altered fibroblast function following myocardial infarction. *J Mol Cell Cardiol*. 2005; 39:699–707.
27. Frangogiannis NG. The mechanistic basis of infarct healing. *Antioxid Redox Signal*. 2006;8:1907–1939.
28. Ertl G, Frantz S. Healing after myocardial infarction. *Cardiovasc Res*. 2005;66:22–32.
29. Hutchins GM, Bulkley BH. Infarct expansion versus extension: two different complications of acute myocardial infarction. *Am J Cardiol*. 1978;41:1127–1132.
30. Cleutjens JP, Blankesteijn WM, Daemen MJ, Smits JF. The infarcted myocardium: simply dead tissue, or a lively target for therapeutic interventions. *Cardiovasc Res*. 1999;44:232–241.
31. Brown RD, Ambler SK, Mitchell MD, Long CS. The cardiac fibroblast: therapeutic target in myocardial remodeling and failure. *Annu Rev Pharmacol Toxicol*. 2005;45:657–687.
32. Jugdutt BI, Musat-Marcu S. Opposite effects of amlodipine and enalapril on infarct collagen and remodelling during healing after reperfused myocardial infarction. *Can J Cardiol*. 2000;16:617–625.
33. Blankesteijn WM, van Gijn ME, Essers-Janssen YPG, Daemen MJAP, Smits JFM. Beta-catenin, an inducer of uncontrolled cell proliferation and migration in malignancies, is localized in the cytoplasm of vascular endothelial cells during neovascularization after myocardial infarction. *Am J Pathol*. 2000;157:877–883.
34. Franco CA, Liebner S, Gerhardt H. Vascular morphogenesis: a Wnt for every vessel? *Curr Opin Genet Dev*. 2009;19:476–483.
35. Jugdutt BI. Limiting fibrosis after myocardial infarction. *N Engl J Med*. 2009;360:1567–1569.

CLINICAL PERSPECTIVE

Myocardial infarction is one of the major causes of heart failure. The scar in the infarct area shows a progressive thinning in these patients, causing excessive dilatation of the entire left ventricle, which leads to pump failure. This dilatation can be attributed to the repetitive mechanical strain that the cardiac cycle places on the scar, causing wear of the extracellular matrix in the scar tissue. Previous work from our laboratory and others has highlighted the importance of myofibroblasts in the maintenance of this scar: The smooth muscle-like contractile properties of these cells provide a sustained contractile force that is subsequently anchored by the deposition of extracellular matrix. In this article, we propose the targeting of myofibroblasts as a novel therapeutic approach to prevent infarct-related heart failure. We have shown previously that myofibroblasts in the infarct area express Frizzled receptors. The receptors use Wnt proteins as their endogenous ligands. Here we describe a fragment of Wnt5a, named UM206, that blocks the interaction between Wnt and Frizzled with high affinity. When administered to infarcted mice, UM206 completely prevented heart failure development. Moreover, infarct thinning and left ventricular dilatation were significantly reduced by UM206, which may be explained by a 4-fold increase in myofibroblast numbers in the infarct area. This study shows that Frizzled blockers may be a novel drug class that can prevent heart failure development after myocardial infarction.

Extended Methods

Western blotting

For Western blot, cells were homogenized in ice-cold Laemmli buffer and protein content was measured using the BCA protein assay (Pierce Biotechnology Inc., Rockford IL, USA); proteins were denatured by boiling, separated on a 10% SDS-page gel, and transferred onto a Hybond C nitrocellulose membrane (Amersham Biosciences, Little Chalfont, United Kingdom). After blocking, membranes were incubated overnight at 4°C with primary antibodies against β-catenin, α-SMA (both 1:2000, BD Biosciences, Franklin Lakes NJ, USA) or β-actin (1:2000 Sigma-Aldrich). Anti-mouse immunoglobulin G 1/5000 (Vector Labs Inc.) was used as the secondary antibody, and the membranes were developed using the Supersignal West Pico chemiluminescence kit (Pierce). Images of the blots were analyzed with image analysis software (Qwin Leica, Cambridge, United Kingdom).

Echocardiography

All mice were subjected to repeated echocardiographic assessment of wall thickness, LV cavity dimensions and ventricular function. Echocardiograms were recorded with Philips Sonos 5500 ultrasound system (Philips, Eindhoven, the Netherlands) using a 20-MHz linear probe under light isoflurane anaesthesia (2%).

Hemodynamic measurements

The animals were anaesthetized with urethane (2.5 mg/g body weight, i.p., Sigma-Aldrich). Mice were intubated and connected to a rodent ventilator (Hugo Sachs, March-

Hugstetten, Germany). Body temperature was maintained at 37°C. The mice were then allowed to stabilize prior to hemodynamic measurements. A high-fidelity catheter tip micromanometer (Mikro-tip1.4F, SPR-671; Millar Instruments, Houston TX, USA) was inserted through the right carotid artery into the left ventricular cavity. Ventricular pressure was measured. Maximal positive and negative pressure development (+dP/dt and –dP/dt) and heart rate were determined on a beat-to-beat basis. The heart was then stimulated by an i.v. ramp-infusion of dobutamine (Sigma-Aldrich, dose range 20-100 μg) using a micro-injection pump (Model 200 Series, KdScientific, Boston, MA, USA).

Peptide Fragment Synthesis

All peptide fragments were synthesized by manual solid-phase peptide synthesis on a 0.3-0.4 mmol scale using the in situ neutralization/activation procedure for Boc-/Bzl- peptide synthesis as previously described [42], but using HCTU instead of HBTU as a coupling reagent. MBHA-polystyrene resin (1 meq/g) was used as the solid support. The peptides were deprotected and cleaved from the resin by treatment with anhydrous HF for 1 h at 0° C, using 4 vol-% p-cresol as a scavenger.

Following cleavage, the peptides were precipitated with ice-cold diethylether, dissolved in aqueous buffer containing 6 M Gn.HCl, 0.1 M sodium acetate buffer (pH 4) and purified by semi-preparative reversed-phase HPLC. Fractions containing the desired product were identified by ESI-MS, pooled and lyophilized.

HPLC

To determine the plasma concentration of UM206, reached by subcutaneous infusion with the minipumps, blood samples were collected from the animals after 14-35 days treatment. Blood was centrifuged and the plasma was treated with 1% TFA. Analytical HPLC was performed using a Vydac C18 RP-HPLC column (4.6 mm × 150 mm, 1 mL/min flow rate) connected to a Varian Prostar system consisting of two Varian Prostar 215 delivery modules and a Varian Prostar 320 UV/vis detector (214 nm). A linear gradient of 0-67% buffer B in buffer A over 30 minutes was used, where buffer A = 0.1 v-% TFA in H_2O and buffer B = 0.1 v-% TFA, 10 v-% H_2O in CH_3CN.

Semi-preparative HPLC was performed using Vydac C18 RP-HPLC columns (10 mm × 250 mm, 5 mL/min flow rate or 22 mm x 250 mm, 10 mL/min flow rate) connected to a Waters Deltaprep System consisting of a Waters Prep LC Controller and a Waters 2487 Dual wavelength Absorbance Detector (214 nm). Peptides were eluted using a shallow gradient of B in A, based on an exploratory analytical HPLC run.

HUVEC isolation and culture

Primary human umbilical vein endothelial cells (HUVECs) were isolated by infusion of trypsin into the umbilical vein which was first washed 3 times by perfusion of PBS. Following trypsin incubation for 20 minutes at 37°C, the cells were collected in HUVEC culture medium (RPMI (Invitrogen) containing 10% fetal calf serum (Invitrogen) and 10% human serum, supplemented with L-glutamin (Invitrogen) and penicillin/streptomycin (Invitrogen)). Next, the trypsin/collection medium mixture was removed by centrifugation for 5 minutes at 400 g. The cells were resuspended in fresh HUVEC culture medium and allowed to adhere for 1 hour at 37°C/5% CO2 in culture

flasks coated with 0.2% gelatine/PBS. Finally, unattached cells and erythrocytes were removed by stringent washing with PBS. Cells were maintained in HUVEC medium at 37°C/5% CO2 and passaged 1:3 upon confluence.

HUVEC proliferation

Proliferation analysis of HUVEC was performed using the CellTiter-Glo® Luminescent Cell Viability Assay (Promega). In brief, cells were plated in gelatin coated 96-wells plates at a density of 5000 cells/well. Next, standard culture medium was replaced with starvation medium (1% HS/1%FCS) and cells were treated for 3 days with the different compounds at the indicated concentrations. Following the treatment period, CellTiter-Glo® analysis was performed according to the suppliers protocol and luminescence was recorded on a Tecan Infinite F200 multimode microplate reader (Tecan Group Ltd.). All treatment conditions were performed in triplicate on three different primary HUVEC isolations.

HUVEC migration

Migration of HUVEC was analyzed using the scratch wound assay. In brief, cells were plated in gelatin coated 96-wells plates at a density of 5000 cells/well. Following three days of growth in standard culture medium the endothelial cell monolayer was scratched using the HTSScratcher (Peira) and medium was replaced with starvation medium (1% HS/1%FCS) containing the different compounds at the indicated concentrations. Images of each scratch were automatically acquired at t = 0 and t = 6 hours with a 1.4 Mb GiGE color camera (Hitachi) on a DMI3000B microscope equipped with an automated xyz-

stage (Leica) using Universal Grab software (version6.3, DCIlabs). Scratch area was determined using Scratch Assay software (version6.2, DCIlabs). All treatment conditions were performed in triplicate on three different primary HUVEC isolations.

Figure legends

Fig. S1: UM206 completely blocks the Wnt3a-induced luciferase activity in CHO (A) and COS-7 (B) cells, transiently transfected with a TopFlash construct. rFzd-1 and -2 were transfected into these cells as indicated.

Fig. S2: Plasma concentration-time curve of a single intravenous bolus injection of 15 microgram of UM206 in the tail vein of mice (N = 24). The plasma half-life was 84 ± 2 min

Fig. S3: Effect of late onset of UM206 treatment on the hemodynamic parameters. UM206 treatment (6 µg/kg.day, subcutaneous administration by osmotic minipump, n=8 per group) was started at 2 weeks after MI and continued until the end of the 5 week experiment. Please note that the effect of the late onset UM206 treatment was comparable to the full 5-week treatment depicted in Fig. 4.

Fig. S4: Administration of UM206 for 5 weeks results in a significant increase in the expression of Collagen Iα1 (Col I*a*1) and a significant decrease in the expression of Collagen III (Col III). *** P<0.001

Fig. S5: Effect of UM206 on Human Umbilical Vein endothelial cell (HUVEC) proliferation and migration. HUVEC proliferation was stimulated by Wnt3a (1.10^{-8} M), and this effect was not blocked by UM206, whereas the anti-angiogenic peptide Anginex (1.10^{-5} M) caused a clear attenuation of the proliferation. Stimulation with 20% human

serum (HS) was used as positive control. UM206 by itself did not affect HUVEC migration, which was stimulated by 20% HS. The combination of UM206 and Wnt3a even caused an attenuation of HUVEC migration. From these data we conclude that UM206 has no direct stimulatory effect on angiogenesis.

Fig S6: Expression levels of different Fzd subtypes in the infarct area, 5 weeks after induction of MI. Please note that MI induces an increase in the expression of Fzd-1 and -2 and that this effect is augmented by UM206 administration

Fig S7: Effect of UM206 treatment on the expression of Wnt proteins in the infarct area, 5 weeks after MI. Administration of UM206 almost completely returns the expression of Wnt3a and 5a, upregulated by MI, to the levels observed in sham animals.

Fig. S8: Binding of UM206-Rhodamine to Frizzled-1 and -2 can be blocked by UM207 and Wnt3a. **A.** Fluorescent signal of UM206-Rhodamine binding to small intestine and kidney is shown in red; green represents autofluorescence of blood vessels in the tissue. **B.** Small intestine and kidney imaging after pre-incubation with UM207 (100 nM) **c.** Small intestine and kidney after pre-incubation with the natural ligand Wnt3a (10 nM). Bar represents 100 μm.

Table S1

Genes	Primers forward	Primers reverse
α-actin	CAGCTGAGAGGGAAATCGTG	CGTTGCCAATAGTGATGACC
Ascl-2	AAGCACACCTTGACTGGTACG	AAGTGGACGTTTGCACCTTCA
α-SMA	AACTGGTATTGTGCTGGACTCTGG	CACGGACGATCTCACGCTCAG
Axin 2	TGACTCTCCTTCCAGATCCCA	TGCCCACATAGGCTGACA
CD 44	TCTGCCATCTAGCACTAAGAGC	GTCTGGGTATTGAAAGGTGTTAGC
Collagen I	TCGATTCACCTACAGCACGC	GACTGTCTTGCCCCAAGTTCC
Collagen III	TCCTGAACATGTCCTTTGATGTA	TTCAGAGACTTCTTTACATTGCCATT
Cyclophilin	TTCCTCCTTTCACAGAATTATTCCA	CCGCCAGTGCCATTATGG
Dickkopf 1	TAGTCCCACCCGCGGAGGGGA	CTTCTGGAATACCCATCCAA
Dickkopf 2	GGATCTTCAGCCTGCATGGT	GGGCAACACATCCCATCTCT
Dickkopf 3	TCAGGAGGAAGCTACGCTCAA	GGTCACCTCAGAGGACGTTCTAG
Dvl 2	ACTGGTGCGGTCTAGGTTTTGA	GGAAGACGTGCCCAAGGA
Fibronectin	TGTCACCCACCACCTTGA	CTGATTGTTCTTCAGTGCGA
Fibronectin ED-A	ACCATTGAAGGTTTGCAACC	GGAGGTGCTGTCTGGAGAAA
Fibronectin ED-B	AGAATAACCACCACCCCCA	TGTTAGGACCACGGCGTT
Inos	CATCCAGAGTGAGCTGGTAGG	GCTGGTAGGGGCAAAAATAGAGGAACATCT
Itm 2A	AGGAGAGCCATACTTTCTGCC	GCCGGATCGCTATCAGAGAGA
LEF	CACACATCCCGTCAGATGTC	TGATGGGATAAACAGGCTGA
MMP 7	CTGCCACTGTCCCAGGAAG	GGGAGAGTTTTCCAGTCATCG
Twist	CTCGGACAAGCTGAGCAAG	ACGGAGAAGGCGTAGCTGAG

Fig. S1

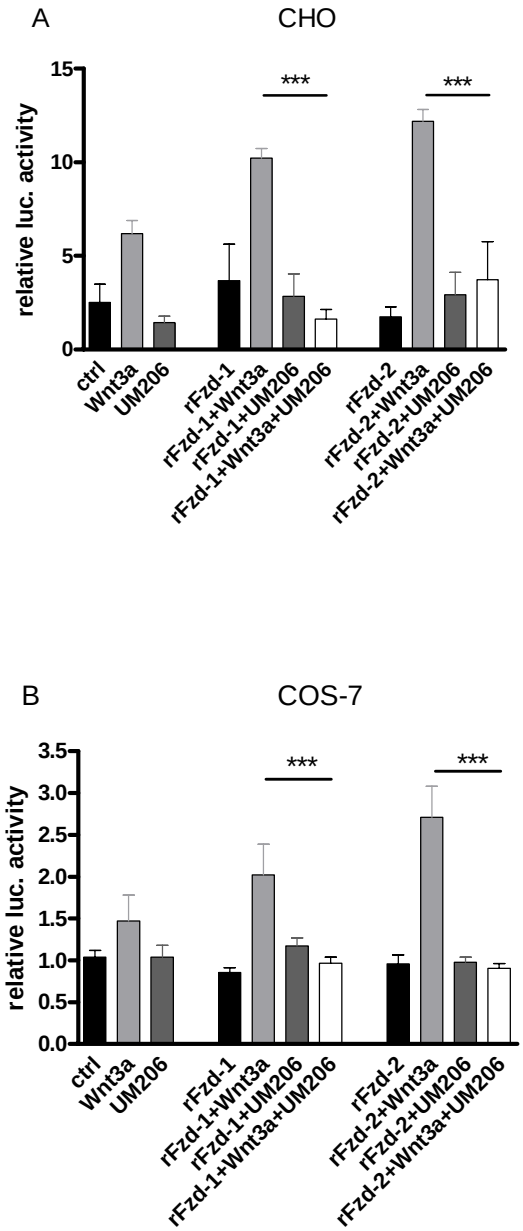

Table S2

	sequence
Peptide 1	Ac-CKCHGVSGSCTVKTCW-NH_2
Peptide 2	Ac-MNRHNNEAGR-NH_2
Peptide 3	Ac-IEECQHQFRDRRWNC-NH_2
Peptide 4	Ac-GDWEWGECSDNI-NH_2
Peptide 5	Ac-DLVYFELSPDFCA-NH_2
Peptide 6	Ac-GSKGTQGRACN-NH_2
Peptide 7	Ac-CNKSGMDGCEL-NH_2

Wnt-derived peptides that were ineffective in antagonizing Fzd-1 and -2

Fig. S2

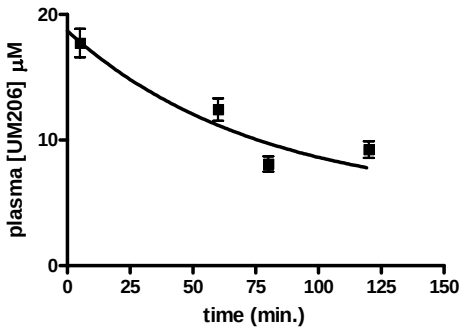

Fig. S3

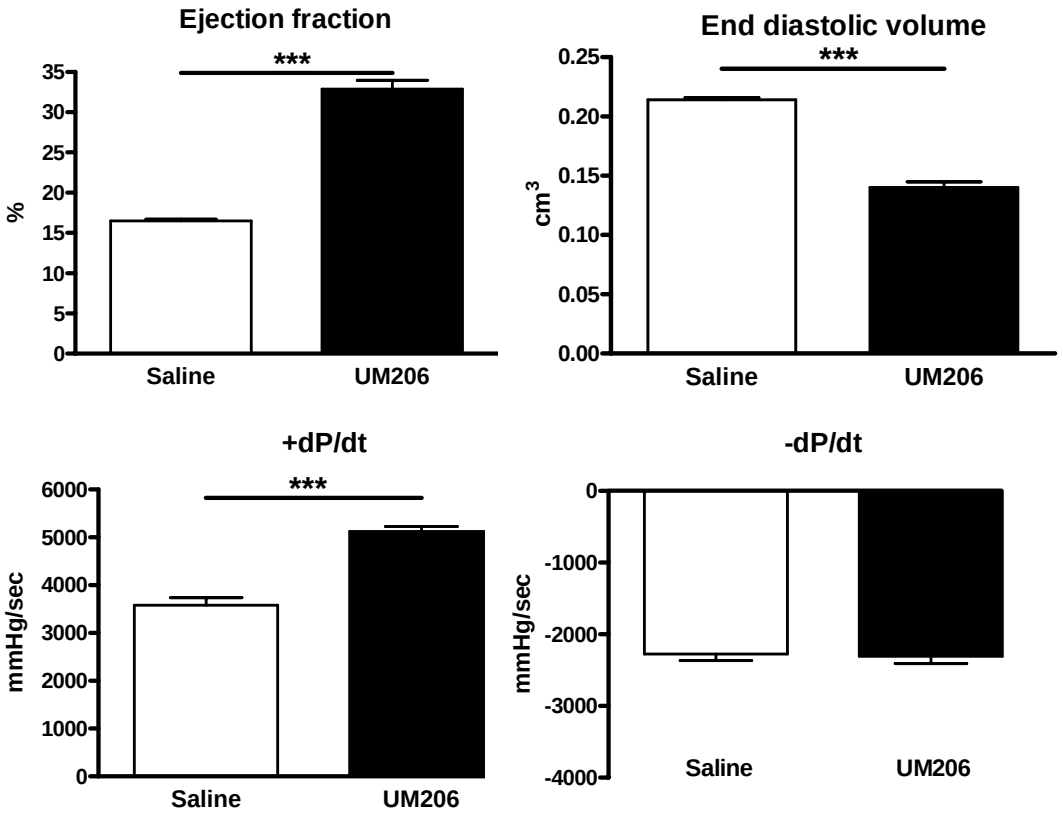

Fig. S4

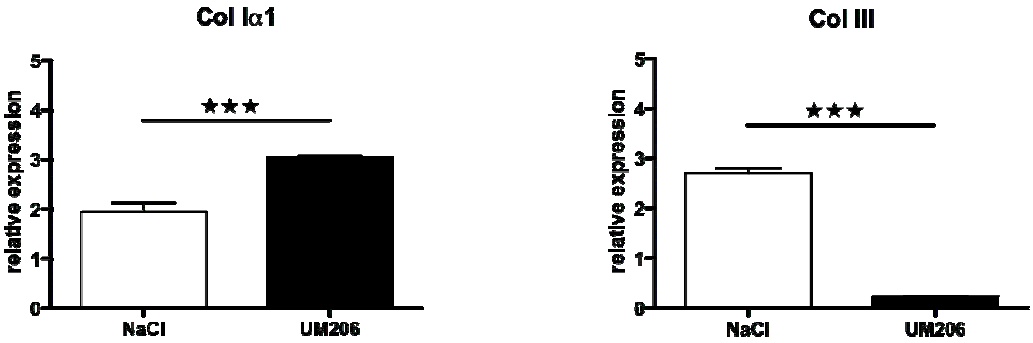

Fig. S5

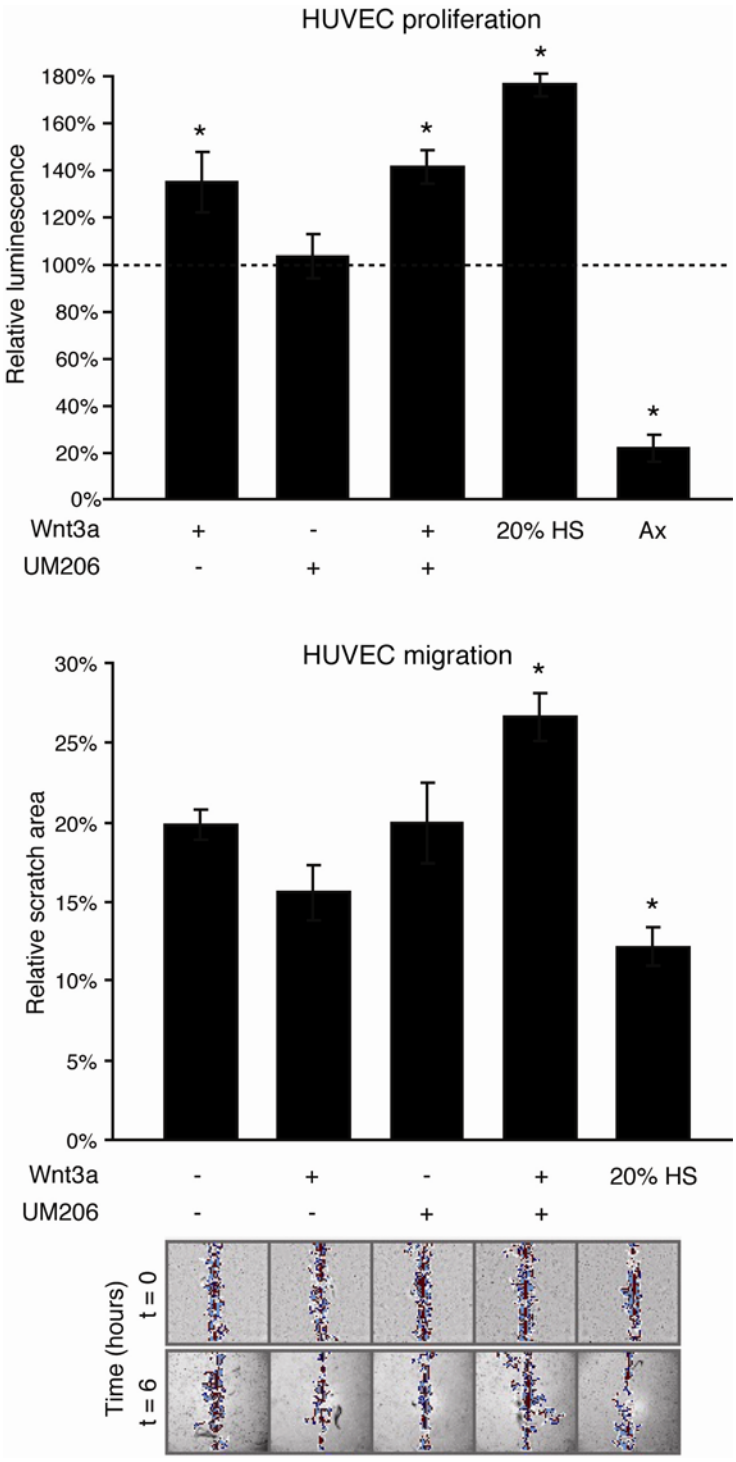

Table S3

small intestine

Gene	Saline		UM206		
	Rel. exp.	SEM	Rel. exp.	SEM	significance
Ascl 2	1.44	0.01	1.42	0.01	-
Dvl 2	1.13	0.03	1.13	0.04	-
Inos	1.19	0.01	1.18	0.02	-
Col I	1.35	0.01	1.32	0.01	-
CD 44	1.27	0.02	1.22	0.02	-
Axin 2	1.08	0.04	1.05	0.04	-
Itm 2A	0.99	0.05	0.97	0.05	-
Mmp 2	1.34	0.01	1.32	0.01	-

kidney

Gene	Saline		UM206		
	Rel. exp.	SEM	Rel. exp.	SEM	significance
Twist	1.45	0.03	1.49	0.03	-
α-actin	1.04	0.01	1.06	0.02	-
LEF	1.66	0.02	1.70	0.09	-
FN	1.62	0.01	1.66	0.01	-
Col I	1.38	0.03	1.39	0.01	-
α-SMA	1.18	0.03	1.21	0.04	-
DDK 1	1.83	0.01	1.87	0.01	-
DDK 2	1.40	0.01	1.44	0.01	-
DDK 3	0.85	0.01	0.87	0.01	-

Effects of 5 week UM206 treatment on the expression levels of genes in small intestine and kidney, for which the expression is known to be regulated by Wnt signaling. The expression levels were determined by qPCR. None of the investigated genes showed a significant change in expression compared to saline treatment.

Fig. S6

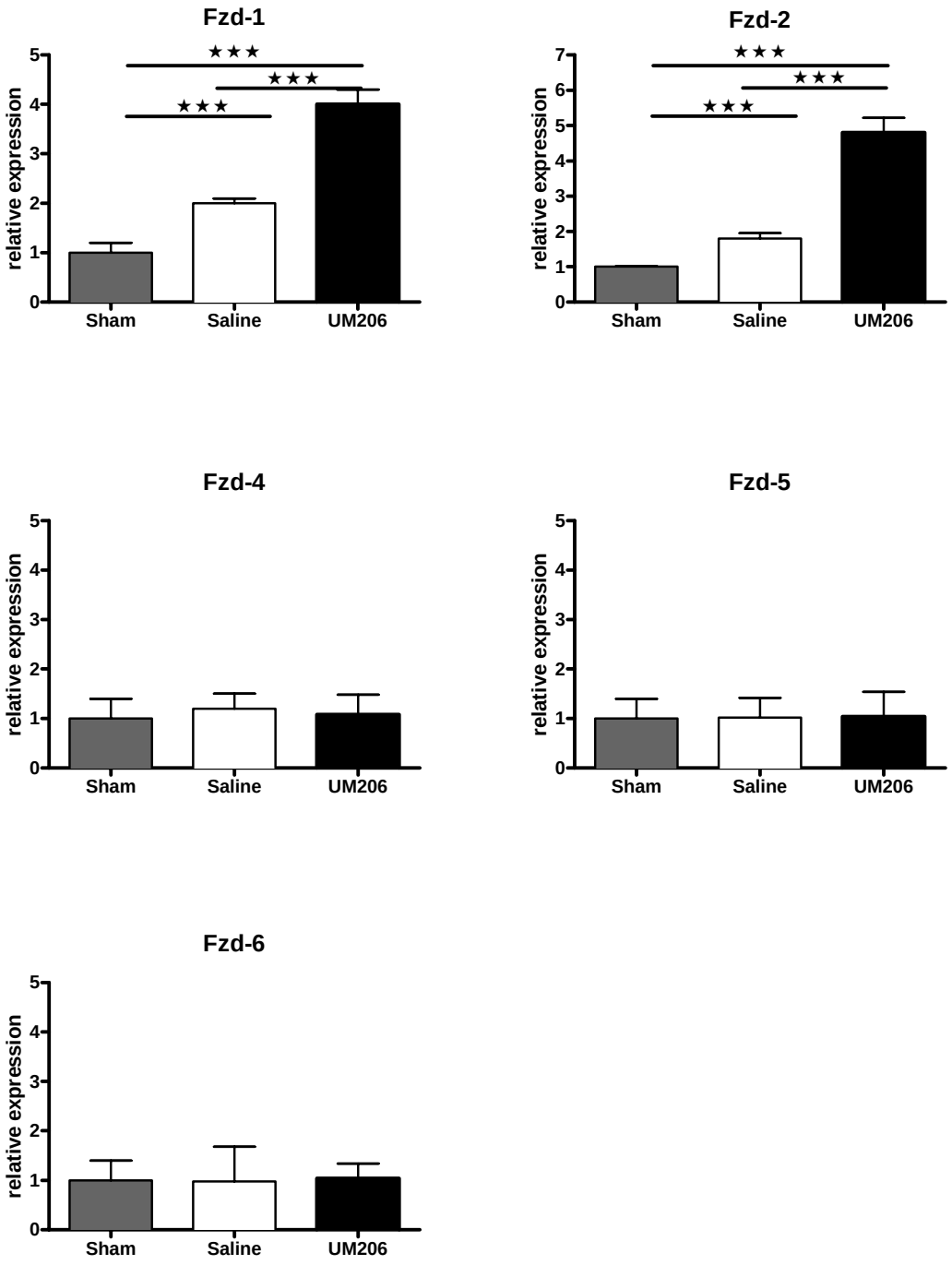

Fig. S7

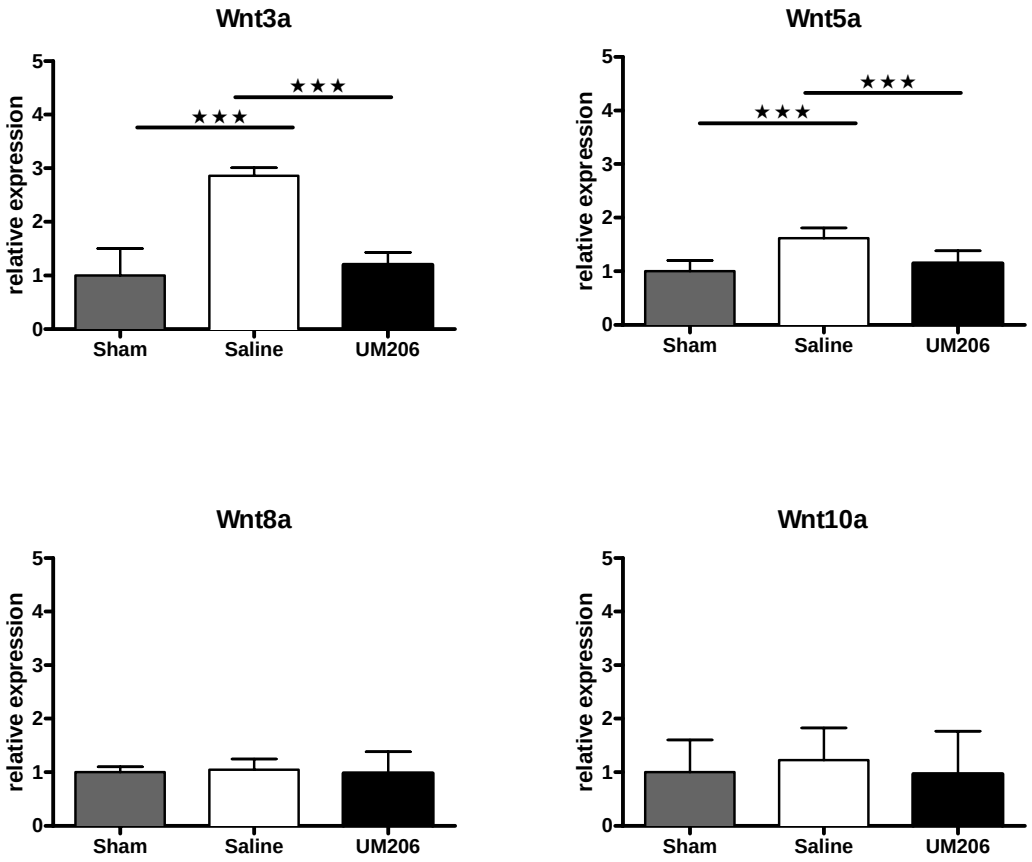

Fig. S8

A UM206-Rhodamine

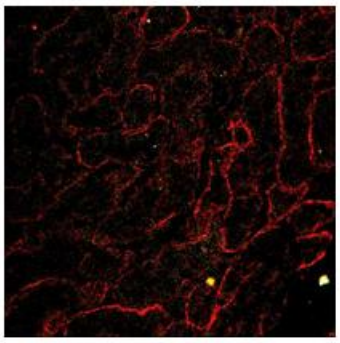

Small intestine

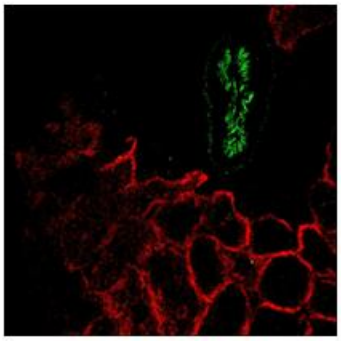

Kidney

B Pre-incubation UM207

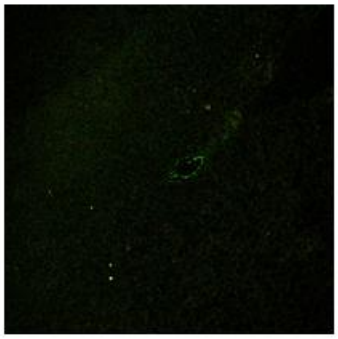

Small intestine

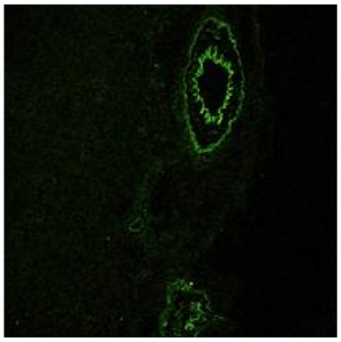

Kidney

C Pre-incubation rWnt3a

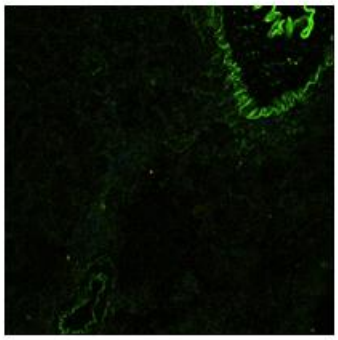

Small intestine

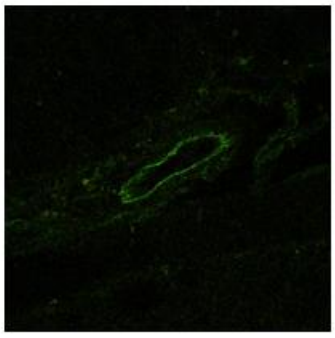

Kidney